Inorganic Chemistry

Article

pubs.acs.org/IC

Understanding Pd−Pd Bond Length Variation in (PNP)Pd−Pd(PNP) Dimers

Justin R. Walensky,[†] Claudia M. Fafard,[‡] Chengyun Guo,[‡] Christina M. Brammell,[†] Bruce M. Foxman,[‡] Michael B. Hall,*[,†] and Oleg V. Ozerov*[,†]

[†]Department of Chemistry, Texas A&M University, 3255 TAMU, College Station, Texas 77842, United States

[‡]Department of Chemistry, Brandeis University, MS 015, 415 South Street, Waltham, Massachusetts 02454, United States

Supporting Information

ABSTRACT: Analysis of the structures of three (PNP)Pd−Pd(PNP) dimers [where PNP stands for anionic diarylamido/bis(phosphine) pincer ligands] has been carried out with the help of single-crystal X-ray diffractometry and density functional theory (DFT) calculations on isolated molecules. The three dimers under study possess analogous ancillary ligands; two of them differ only by an F versus Me substituent in a remote (five bonds away from Pd) position of the pincer ligand. Despite these close similarities, X-ray structural determinations revealed two distinct structural motifs: a highly symmetric molecule with a long Pd−Pd bond or a highly distorted molecule with Pd−Pd bonds ca. 0.14 Å shorter. DFT calculations on a series of (PNP)Pd−Pd(PNP) dimers (as molecules in the gas phase) confirmed the existence of these distinct minima for dimers carrying large isopropyl substituents on the P-donor atoms (as in the experimental structure). These minima are nearly isoergic conformers. Evidently, the electronically preferred symmetric structure for the dimer (with a square-planar environment about Pd and a linear N−Pd−Pd−N vector) is not sterically possible with the preferred Pd−Pd distance. Thus, the minima correspond to either a symmetric structure with a long Pd−Pd bond distance or a structure with a short Pd−Pd distance but with substantial distortions in the Pd coordination environment to alleviate steric conflict. This notion is supported by finding only a single minimum (symmetric and with short Pd−Pd bonds) for each of the dimers carrying smaller substituents (H or Me) on the P atoms, regardless of the remote substitution.

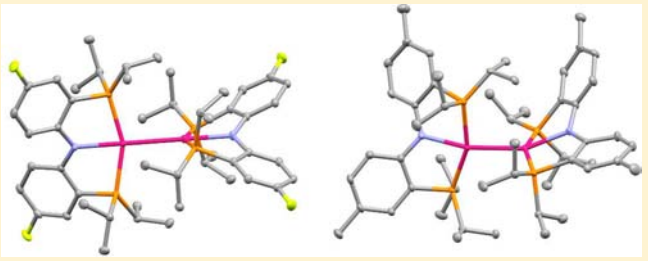

INTRODUCTION

We have previously reported [(PNP)Pd−]$_2$) dimers[1,2] containing an unbridged Pd−Pd single bond and supported by diarylamido/bis(phosphine) PNP[3−5] pincer ligands (Scheme 1). These dimers exhibited unusual reactivity toward small molecules such as O_2 (the formation of palladium superoxide and dipalladium peroxide in equilibrium with free O_2)[1] and NH_3 (splitting of ammonia into Pd−H and Pd−NH_2).[2] The Pd−Pd bond is the pivotal reactive site, and in this work, we present an analysis of a puzzling Pd−Pd bond length variation that we uncovered in the course of structural studies. We were surprised to obtain solid-state structures of three closely related dimers of the general formula [(PNP)Pd−]$_2$) (Scheme 1) that revealed Pd−Pd distances different by a remarkable 0.14 Å with no changes in connectivity and no significant variation of other bond lengths in the molecules. Isomers of compounds that have different interatomic distances based on the presence versus absence of a direct bond between two atoms have been described, although they tend to contain different geometric or electronic features in the ligands, often as a consequence of the ligands being bridged.[6−9] While the different Pd−Pd distances in our present work were observed for nonidentical PNP ligands, and thus not for *isomers*, the PNP ligands in question were similar enough (especially, ^{F}PNP vs ^{Me}PNP in Scheme 1) that we would have a priori expected a negligible variation in the Pd−Pd distances. In this report, we present our structural and computational investigation of the underlying factors responsible for the variable Pd−Pd distances. Indeed, these Pd−Pd bond-length variations are accompanied by other changes, even if they are not obvious from the structures drawn on paper.

EXPERIMENTAL RESULTS

Synthesis and Characterization. The syntheses and isolation of the dimers ^{F}**1** and ^{Me}**1** by photolysis of (^{F}PNP^{iPr})PdEt and (^{Me}PNP^{iPr})PdEt, respectively, were reported previously (Scheme 1). The solid-state structural determination of ^{Me}**1** was reported in the same work. We were able to obtain X-ray-quality single crystals of ^{F}**1** directly by photolysis of a solution of (^{F}PNP^{iPr})PdEt in tetrahydrofuran (THF).

The synthesis of TH**1** carrying the "tied" PNP ligand was undertaken analogously to that of ^{F}**1** and ^{Me}**1**. The reaction of the previously described (THPNP^{iPr})PdCl[10] with Et_2Zn furnished (THPNP^{iPr})PdEt, the photolysis of which produced the new dimer TH**1** (Scheme 1). Compound TH**1** turned out to be considerably more soluble than ^{F}**1** or ^{Me}**1** and was purified and isolated by recrystallization from pentane,

Received: July 25, 2012
Published: February 19, 2013

   dx.doi.org/10.1021/ic301629m | *Inorg. Chem.* 2013, 52, 2317−2322

Scheme 1

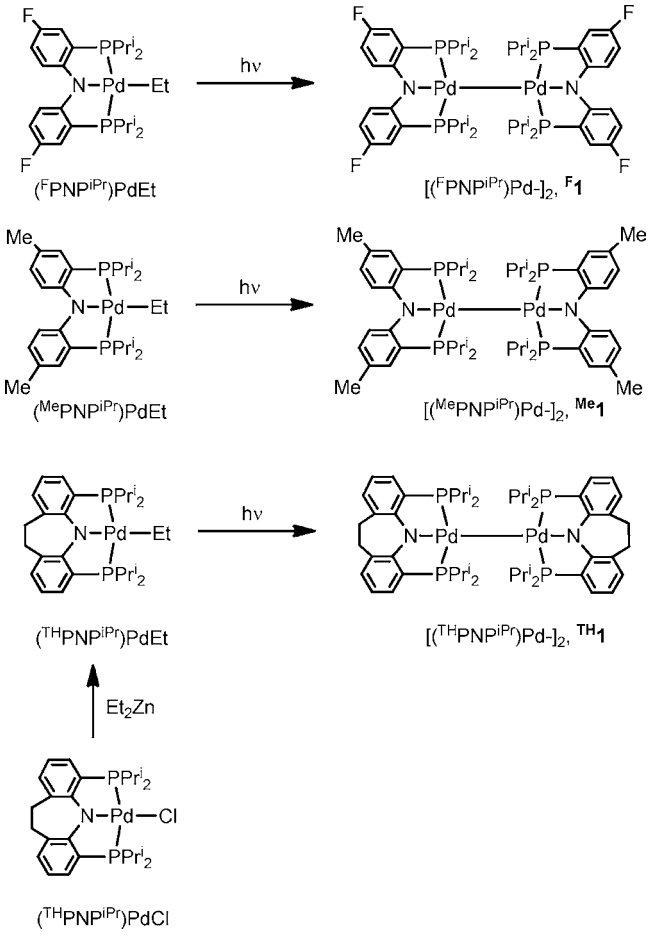

yielding X-ray-quality single crystals. The NMR spectroscopic features of TH**1** at ambient temperature are more complex than those of ^{F}**1** and ^{Me}**1**. Upon cooling to −55 °C, the broad features partly resolve. In the $^{31}P\{^{1}H\}$ NMR spectrum, the dominant signals at −55 °C belong to two AB systems ($^{2}J_{PP}$ = 356 and 358 Hz indicative of *trans* disposition of phosphines), with other minor broad resonances evident. Upon heating a solution of TH**1** to +75 °C, the $^{31}P\{^{1}H\}$ and ^{1}H NMR spectra coalesce into a picture indicative of the same maximal (for a PNP complex) symmetry observed for ^{F}**1** and ^{Me}**1**. It corresponds to D_{2d} symmetry for the dimer molecule or the local C_{2v} symmetry for each constituent "half". While we have not analyzed them in detail, these data are consistent with the notion of multiple low-symmetry conformers of TH**1** interconverting slowly at room temperature on the NMR time scale. The notion of multiple conformers forming distinguishable minima is in line with the overall findings in this work, but we do not have any direct evidence that these conformers of TH**1** necessarily possess very different Pd−Pd distances. That the interconversion among them is slower for TH**1** than for ^{F}**1**/^{Me}**1** is not surprising because it appears that conformational exchanges are, in general, slower with the THPNP ligand, as we observed in past cases.[10,11] This is presumably caused by the restrictions imposed on the conformational space by the ring-linking CH_2CH_2 tether.

X-ray Structural Studies. The solid-state structures of ^{F}**1** and TH**1** were determined by single-crystal X-ray diffraction in this work (Figure 1 and Table 1). These new results complement the previously reported structural determination of ^{Me}**1** (see Table 2 for the summarized crystal data for ^{F}**1**, TH**1**, and ^{Me}**1**).[2] All three dimers contain an unbridged Pd−Pd bond, and the environments about each Pd are best described as distorted square-planar. However, the molecular structures of ^{F}**1**, on the one hand, and ^{Me}**1** and TH**1**, on the other hand, differ from each other in two key respects: (1) the Pd−Pd bond distance and (2) the parameters of distortion from square-planar

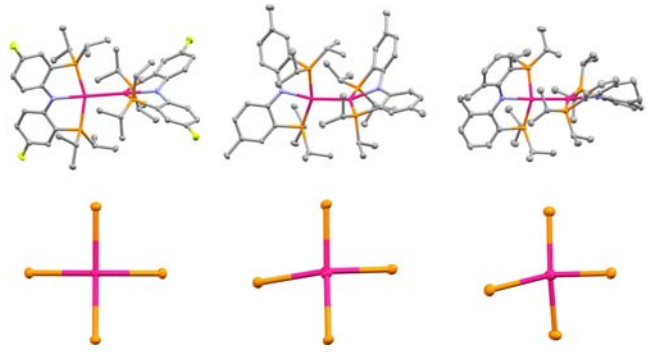

Figure 1. Top: POV-Ray rendition[18] of the ORTEP drawings[19] (50% probability ellipsoids) of the X-ray structures of ^{F}**1** (left), ^{Me}**1** (center), and TH**1** (right) in the solid state. Correspondence of color to elements: C, gray; F, yellow-green; N, blue; P, orange; Pd, magenta. H atoms in all structures, as well as the two pentane solvent molecules and the disorder in one of the isopropyl groups in TH**1**, are omitted for clarity. Bottom: View of the cores of the structures of ^{F}**1** (left), ^{Me}**1** (center), and TH**1** (right) along the Pd−Pd axis with only the Pd and P atoms shown.

Table 1. Selected Bond Distances (Å), Angles (deg), and Dihedral Angles (deg) from the Solid-State X-ray Studies of ^{F}1, ^{Me}1, and TH1

metric (Å or deg)	^{F}**1**	^{Me}**1**	TH**1**
Pd−Pd	2.7167(2)	2.5758(4)	2.5844(2)
N−Pd	2.1647(12)	2.121(3)	2.1821(18)
		2.122(3)	2.1976(17)
P−Pd	2.3148(2)	2.2967(9)	2.2742(6)
		2.3301(9)	2.2966(6)
		2.3135(10)	2.2763(6)
		2.2965(10)	2.2835(6)
P−Pd−P	156.417(13)	158.37(3)	160.10(2)
		155.39(3)	154.81(2)
N−Pd−Pd	180	165.67(9)	167.64(5)
		157.70(8)	158.57(5)
N−Pd−Pd−N	0	31.70	17.04

geometry. It is worth noting that the structure of ^{F}**1** was determined multiple times via X-ray studies of single crystals of different batches.

As we previously discussed,[2,12] the effective covalent radius of a (PNP^{iPr})Pd fragment can be taken at ca. 1.29 Å by subtraction of 0.77 Å (covalent radius of CH_3 as half the C−C distance in ethane) from the Pd−CH_3 distance in ($^{F}PNP^{iPr}$)PdMe.[13] The expected Pd−Pd distance for the dimer is thus ca. 2.58 Å. The Pd−Pd bond distances in compounds ^{Me}**1** and TH**1** agree well with this predicted value. The distances are also similar to the ca. 2.60 Å Pd−Pd bond distances in $[(Me_3P)_3Pd{-}Pd(PMe_3)_3]^{2+}$ (unbridged Pd^{I}−Pd^{I} bond) and in $[(\mu\text{-}Me_2PCH_2PMe_2)_2Pd_2Br_2]$ (similar PXP ligand set about each Pd).[14,15] Compounds with shorter Pd^{I}−Pd^{I} distances are known, but they tend to arise in cases with tight-bridging ligands tethering the two Pd centers.[16] Thus, it was rather surprising to discover that compound ^{F}**1** possesses a much longer Pd−Pd bond distance of 2.7167(2) Å. This absolute value for a Pd^{I}−Pd^{I} bond is not unprecedented;[17] what is unusual is its striking ca. 0.14 Å difference with the nearly identical molecule ^{Me}**1**.

The molecular structure of ^{F}**1** in the crystal is more symmetric than the structures of ^{Me}**1** and TH**1**. The bottom half of Figure 1 visually accentuates the differences in the cores of the molecules. To provide a more quantitative measure of the differences, it is important to note that the midpoint of the Pd−Pd vector of ^{F}**1** lies on a crystallographic $\bar{4}$ rotary inversion axis (Wyckoff position b in $I4_1/a$, origin choice 2) and the asymmetric unit consists of a "quarter" of the dimer molecule. The Schönflies point group of the molecule of ^{F}**1** in the crystal is S_4

dx.doi.org/10.1021/ic301629m | *Inorg. Chem.* 2013, 52, 2317−2322

Table 2. Selected Crystal Data for ^{F}1, ^{Me}1, and TH1.[20]

	^{F}1	^{Me}1	TH1
empirical formula	$C_{24}H_{34}F_2N_1P_2Pd_1$	$C_{52}H_{80}N_2P_4Pd_2$	$C_{62}H_{100}N_2P_4Pd_2$
fw (g mol^{-1})	542.88	1069.92	1210.18
cryst syst	tetragonal	triclinic	monoclinic
space group	$I4_1/a$	$P\bar{1}$	$P2_1/c$
a (Å)	17.6501(4)	11.2634(5)	18.5297(7)
b (Å)	17.6501(4)	13.2400(6)	14.9059(6)
c (Å)	15.1012(7)	16.9092(8)	21.7591(8)
α (deg)	90	83.795(2)	90
β (deg)	90	86.868(2)	95.862(2)
γ (deg)	90	85.173(2)	90
V (Å^3)	4704.4(3)	2495.3(2)	5978.5(4)
Z, Z'	8, 0.5	2, 1	4, 1
ρ_{calcd} (Mg m^{-3})	1.533	1.424	1.344
abs coeff (mm^{-1})	0.952	0.885	0.748
F(000)	2232	1116	2552
cryst size (mm^3)	0.450 × 0.340 × 0.302	0.36 × 0.19 × 0.06	0.438 × 0.196 × 0.097
θ_{min} (θ_{max}) (deg)	1.775 (30.046)	1.552 (30.225)	1.659 (28.331)
no. of reflns (indep)	53092 (3456)	27999 (14484)	98551 (14783)
R_{int}	0.037	0.043	0.051
completeness to θ_{max} (%)	100	98.8	100
data/restraints/param	3456/0/137	14469/0/541	14734/1/631
R1 [$I > 2\sigma(I)$]	0.0148	0.0414	0.0294
wR2 (all data)	0.0390	0.1181	0.0698
GOF	0.99	0.98	0.99
largest diff peak/hole	0.44/−0.29	1.01/−1.02	1.94/−2.13

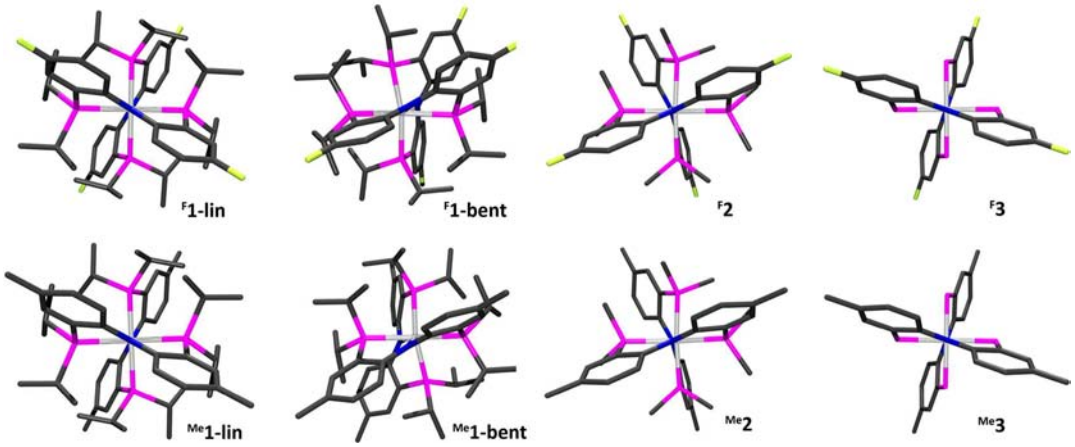

Figure 2. Top: POV-Ray[18] rendition of the rod drawings of the calculated structures viewed along the Pd−Pd axes. Correspondence of color to elements: C, dark gray; F, yellow-green; N, navy blue; P, magenta; Pd, gray metallic. H atoms in all structures are omitted for clarity.

[or C_2 for each (PNP)Pd "half"]. This means that all four P atoms and the associated distances and angles are crystallographically equivalent, each Pd lies in the plane defined by its four P, N, P, and Pd donor atoms, the two (PNP)Pd planes are perpendicular to each other, and the N−Pd−Pd−N linkage is linear. In contrast, in both ^{Me}**1** and TH**1**, none of the N−Pd−Pd angles are 180° and the Pd atoms deviate significantly from the planes defined by any three of their donor atoms. The other angles centering on Pd in each molecule of ^{Me}**1** and TH**1** are all different but not to an extent that demands interpretation. The distortion from the square plane about the Pd centers in ^{Me}**1** and TH**1** is of a seesaw type, whereas in ^{F}**1**, the only distortion is the <180° P−Pd−P angle owing to the constraint of the pincer backbone, uniformly observed in monometallic (PNP)PdX compounds.

Computational Studies. The differences in the observed solid-state structures are dramatic for an apparently immaterial change in the ligand. ^{F}**1** and ^{Me}**1** differ only by the F versus Me substituent para to the N in the diarylamido backbone, and it was difficult to envisage how this remote, sterically irrelevant, and electronically modest variation can be responsible for the ca. 0.14 Å(!) elongation of the Pd−Pd bond distance. We decided to use density functional theory (DFT) to analyze the structural preferences of the Pd dimers in question. We left complex TH**1** out of the computational study because its structure is qualitatively similar to that of ^{Me}**1** and focused on the more straightforward comparison between ^{F}**1** and ^{Me}**1**. Our objectives for this study may be formulated in terms of seeking the answers to two questions: (1) Is the difference in the solid-state structure reflective of the structural preferences of isolated molecules? (2) Why are there two possible structures with rather dramatic differences?

Is the Difference in the Solid-State Structure Reflective of the Structural Preferences of Isolated Molecules? We used the experimentally determined structures of ^{F}**1** and ^{Me}**1** as the starting points in the calculations. In both cases, convergence to a minimum closely resembling the experimental structure was easily achieved: linear for ^{F}**1** and bent for ^{Me}**1**. From here on, we will refer to the

dx.doi.org/10.1021/ic301629m | Inorg. Chem. 2013, 52, 2317−2322

Table 3. Selected Bond Distances (Å), Angles (deg), and Dihedral Angles (deg) from the DFT-Calculated Structures of ^{F}1, ^{Me}1, ^{F}2, ^{Me}2, ^{F}3, and ^{Me}3

metric (Å or deg)	^{F}1-lin	^{F}1-bent	^{Me}1-lin	^{Me}1-bent	^{F}2	^{Me}2	^{F}3	^{Me}3
Pd–Pd	2.814	2.669	2.815	2.669	2.596	2.598	2.575	2.575
N–Pd	2.213	2.180	2.215	2.181	2.173	2.173	2.166	2.168
		2.188		2.190	2.175	2.178		
P–Pd	2.393	2.370	2.393	2.370	2.318	2.315	2.293	2.293
		2.384		2.383	2.320	2.318		
		2.355		2.356	2.316	2.320		
		2.399		2.399	2.320	2.321		
P–Pd–P	155.12	151.93	155.03	151.92	162.16	161.80	164.86	164.84
		157.79		157.58	163.09	163.28		
N–Pd–Pd	180	155.98	180	156.06	173.36	172.34	180	180
		168.80		168.66	176.10	175.59		
N–Pd–Pd–N	0	24.58	0	24.52	11.92	2.11	0	0

structure experimentally determined for ^{F}1 as "linear" and that for ^{Me}1 as "bent" and will abbreviate them as ^{F}1-lin and ^{Me}1-bent, respectively. Then, we computationally "replaced" the F atoms in ^{F}1-lin with Me groups and the corresponding Me groups in ^{Me}1-bent with F atoms and performed geometry optimization again. In this case, as well, convergence to the minima closely resembling the starting points was achieved for both structures: ^{Me}1-lin and ^{F}1-bent. The graphical representation of these computed structures is shown in Figure 2, and the metric data are collected in Table 3.

The agreement between the calculated structures ^{F}1-lin and ^{Me}1-bent and the experimentally determined structures for ^{F}1 and ^{Me}1 was very reasonable. The calculated bond distances were consistently longer, but that was an expected result for the B3LYP functional. The overestimation of the bond lengths was the greatest in absolute terms for the Pd–Pd bonds, which were calculated to be ca. 0.09 Å longer than those in the X-ray diffraction studies. The angles associated with Pd were reproduced more faithfully. However, most importantly, the calculated structures recognizably reproduced the difference in the symmetry of ^{F}1-lin and ^{Me}1-bent and the associated dramatic difference in the Pd–Pd bond distance.

For both ^{F}1 and ^{Me}1, the linear structure is calculated to be 1.6 and 0.6 kcal mol^{-1}, respectively, lower in energy than the analogous bent conformation, a very small difference, albeit slightly greater for ^{F}1. The structural parameters calculated for the two bent structures ^{F}1-bent and ^{Me}1-bent are nearly identical; the same correspondence was evident in the pair of linear calculated structures ^{F}1-lin and ^{Me}1-lin. On the basis of these findings, it must be concluded that the choice of F versus Me substituent does not control the different preference for bent versus linear in separate molecules. The best explanation of the experimental observation of differing solid-state structures for ^{F}1 and ^{Me}1 appears to be that the difference in energy for the bent and linear forms is small and the structural preference of an isolated molecule may be overridden by the sum of the weak intermolecular contacts in the three-dimensional crystal lattice.

Why Are There Two Different Structures? To shed light on this question, we used DFT to optimize the structures of dimers with PNP ligands of reduced steric bulk (Figures 2 and 3 and Table 2): ^{F}2 and ^{Me}2, carrying PMe_2 donors, and ^{F}3 and ^{Me}3, carrying PH_2 donors. For each of these four structures, convergence to a single minimum was achieved, regardless of whether the calculation started from a linear or bent initial input structure. For ^{F}3 and ^{Me}3, the optimized structures are strictly linear. For ^{F}2 and ^{Me}2, they are slightly bent, but not nearly to the extent observed in ^{F}1-bent and ^{Me}2-bent. However, the calculated Pd–Pd distance in ^{F}2 and ^{Me}2, and especially ^{F}3 and ^{Me}3, is quite short, more than 0.2 Å shorter than that calculated for ^{F}1-lin/^{Me}2-lin but also ca. 0.07–0.10 Å shorter than that calculated for ^{F}1-bent/^{Me}2-bent.

It seems reasonable to conclude that the intrinsic *electronic* preference is for a symmetric, linear structure. The bent structure is then a compromise between maintaining a shorter Pd–Pd bond and minimizing the steric repulsion between the two PNP ligands through angular distortions. For the full ^{F}PNP^{iPr} ligand in ^{F}1, the linear structure is sterically only possible with a much longer Pd–Pd bond.

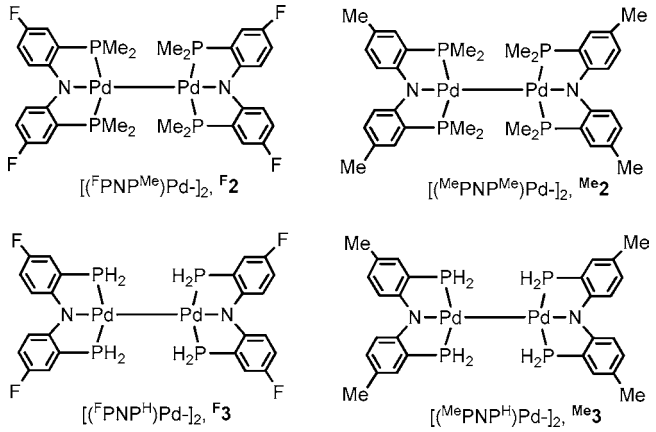

Figure 3. Dimer molecules with PMe_2 (^{F}2 and ^{Me}2) and PH_2 (^{F}3 and ^{Me}3) pincer side arms used in DFT calculations.

CONCLUSION

In summary, we have determined solid-state X-ray structures of three Pd^{I}–Pd^{I} dimers supported by three different, but closely analogous, PNP pincer ligands. These structures display a surprisingly large variation in the Pd–Pd bond length, in spite of nearly identical connectivity and apparent steric and electronic properties of the ligands. Computational analysis of a series of Pd–Pd dimers indicates that variation of the Pd–Pd bond distances arises from the interplay between the steric repulsion between the supporting pincer ligands and the innate electronic preferences of the Pd–Pd bond.

EXPERIMENTAL SECTION

Computational Details. All B3LYP[21] (Becke-3 exchange[22] and Lee–Yang–Parr correlation[23] functional) calculations were performed using the *Gaussian 09* suite of software.[24] Full geometry optimizations were performed and stationary points were characterized via analytical frequency calculations using the Pople double-ζ quality basis set [6-31G(d′)][25] for the C, H, and N atoms, which contains a polarization (d) function on the C, N, and O atoms. The Stuttgart/Dresden triple-ζ quality basis set with an effective core potential[26] for the Pd and P atoms was employed with an additional d basis function with an exponent of 0.387 on P.

General Experimental Considerations. Unless specified otherwise, all manipulations were performed under an argon atmosphere using standard Schlenk or glovebox techniques. Dioxane, diethyl ether,

dx.doi.org/10.1021/ic301629m | Inorg. Chem. 2013, 52, 2317–2322

THF, and benzene were dried over sodium benzophenone ketyl, distilled or vacuum transferred, and stored over molecular sieves in an argon-filled glovebox; (THPNP^{iPr})PdCl was synthesized according to published procedures,[10] and all other chemicals were used as received from commercial vendors. All NMR spectra were recorded on a Varian iNova 300 spectrometer (^{1}H NMR, 299.951 MHz; ^{31}P NMR, 121.425 MHz; ^{13}C NMR, 75.413 MHz), a Varian Mercury 300 spectrometer (^{13}C NMR, 75.426 MHz), a Varian iNova 400 spectrometer (^{1}H NMR, 399.755 MHz; ^{13}C NMR, 100.518 MHz; ^{31}P NMR, 181.822 MHz), or a Varian iNova NMR 500 spectrometer (^{1}H NMR, 499.425 MHz/499.683 MHz; ^{13}C NMR, 75.424 MHz/125.580 MHz; ^{31}P NMR, 202.171 MHz). Chemical shifts are reported in δ/ppm. For ^{1}H and ^{13}C NMR spectra, the residual solvent peak was used as an internal reference. ^{31}P NMR spectra were referenced externally using 85% H_3PO_4 at δ 0. Elemental analyses were performed by CALI Laboratories, Parsippany, NJ. UV experiments were performed under a 250 W, 130 V tungsten/halogen lamp. The X-ray structural study of ^{Me}**1** was reported previously.[2]

(THPNP^{iPr})PdEt. In a 50 mL Schlenk flask, 87.6 mg (0.153 mmol) of THPNPPdCl was dissolved in toluene. To the flask, was added 165 μL (0.165 mmol) of 1.0 M Et_2Zn in heptane. The flask was covered in aluminum foil, and the solution was stirred overnight at room temperature. The next day the solution was passed through a plug of silica gel and washed with toluene. The yellow filtrate was stripped down. A yellow solid powder was collected. Yield: 54 mg (62%). ^{1}H NMR (C_6D_6): δ 6.88 (dd, J = 1.5, 5 Hz, 2H, Ar−H), 6.84 (d, J = 6 Hz, 2H, Ar−H), 6.46 (t, J = 7 Hz, t, Ar−H), 2.99 (s, 4H, $-CH_2CH_2-$), 2.21 (m, 4H, $CHMe_2$), 1.93 (app sextet, 2H, J = 8 Hz, $PdCH_2CH_3$), 1.55 (dt, J = 8 and 3 Hz, 3H, $PdCH_2CH_3$), 1.23 (app q (dvt), 12H, J = 8 Hz, $CHMe_2$), 1.06 (app br q (dvt), 12H, J = 7 Hz, $CHMe_2$). ^{31}P{^{1}H} NMR (C_6D_6): δ 38.8 s. ^{13}C{^{1}H} NMR (C_6D_6): δ 161.4 (vt, J = 12 Hz, C−N), 134.8 (vt, J = 4 Hz), 133.0 (s), 130.6 (s), 121.6 (vt, J_{CP} = 25 Hz), 113.7 (vt, J = 13 Hz), 40.7 (s, $-CH_2CH_2-$), 25.0 (br s, $CHMe_2$), 19.2 (s, $CHMe_2$), 18.4 (s, CH_2CH_3), 17.6 (br s, $CHMe_2$), −5.0 (t, J = 4 Hz, CH_2CH_3).

[(THPNP^{iPr})Pd−]$_2$ (TH1). In a 50 mL poly(tetrafluoroethylene) screw-valve flask, 38.0 mg (0.0676 mmol) of (THPNP^{iPr})PdEt was dissolved in pentane. The flask was placed in front of a UV tungsten, 250 W halogen lamp for 5 days. The solution was then transferred to a Schlenk flask, washed with pentane, and then passed through a plug of Celite. The volatiles were removed from the filtrate in vacuo. Pentane was added to dissolve the residue, and the solution was then placed in a −35 °C freezer for recrystallization. A crystalline solid was collected. Yield: 24 mg (33%). ^{1}H NMR (C_6D_6, +75 °C): δ 6.88 (br, 2H, Ar−H), 6.72 (d, 2H, J = 7 Hz, Ar−H), 6.30 (t, 2H, J = 7 Hz, Ar−H), 2.95 (s, 4H, $-CH_2CH_2-$), 2.31 (m, 4H, $CHMe_2$), 1.35 (app q (dvt), 12H, J = 7 Hz, $CHMe_2$), 1.11 (br, 12H, $CHMe_2$). ^{31}P{^{1}H} NMR (C_6D_6, +75 °C): δ 53.5 s. ^{31}P{^{1}H} NMR (C_6D_6, −55 °C): δ 66.8 (d, J = 356 Hz), 46.2 (d, J = 356 Hz), 44.5 (d, J = 358 Hz), 38.8 (d, J = 358 Hz). Elem anal. Calcd for $C_{52}H_{76}N_2P_4Pd_2$: C, 58.59; H, 7.19. Found: C, 58.66; H, 7.39.

X-ray Data Collection, Solution, and Refinement for [(^{F}PNP^{iPr})Pd−]$_2$ (^{F}1). All operations were performed on a Bruker Nonius-Kappa Apex2 diffractometer, using graphite-monochromated Mo Kα radiation. All diffractometer manipulations, including data collection, integration, scaling, and absorption corrections, were carried out using the Bruker *Apex2* software.[27] Preliminary cell constants were obtained from three sets of 12 frames. Data collection was carried out at 120 K, using a frame time of 10 s and a detector distance of 60 mm. The optimized strategy used for data collection consisted of five ϕ and one ω scan sets, with 0.5° steps in ϕ or ω; completeness was 100.0%. A total of 3654 frames were collected. Final cell constants were obtained from the *xyz* centroids of 9949 reflections after integration.

From the systematic absences and the observed metric constants and intensity statistics, space group $I4_1/a$ was chosen initially; subsequent solution and refinement confirmed the correctness of this choice. The structure was solved using *SIR92* and subsequent electron-density difference syntheses.[28] Refinement (full-matrix least squares) was carried out using the Oxford University *Crystals for Windows* program.[29] All non-H atoms were refined using anisotropic displacement parameters. After location of H atoms on electron-density difference maps, the H atoms were initially refined with soft restraints on the bond lengths and angles to regularize their geometry (C---H in the range 0.93−0.98 Å and U_{iso}(H) in the range 1.2−1.5U_{eq} of the parent atom), after which the positions were refined with riding constraints.[30] The final least-squares refinement converged to R1 = 0.0148 [$I > 2\sigma(I)$; 3223 data] and wR2 = 0.0390 (F^2; 3456 data; 137 parameters). The final CIF file is available as Supporting Information; we note that the CheckCIF routine produced one Alert B item, related to a Hirshfeld test failure in the structure. Accordingly, the CIF file and CheckCIF output contain a validation reply form item that addresses the Alert B item.

X-ray Data Collection, Solution, and Refinement for TH1. All operations were performed on a Bruker Nonius-Kappa Apex2 diffractometer, using graphite-monochromated Mo Kα radiation. All diffractometer manipulations, including data collection, integration, scaling, and absorption corrections, were carried out using the Bruker *Apex2* software.[27] Preliminary cell constants were obtained from three sets of 12 frames. Data collection was carried out at 120 K, using a frame time of 20 s and a detector distance of 60 mm. The optimized strategy used for data collection consisted of three ϕ and two ω scan sets, with 0.5° steps in ϕ or ω; completeness was 99.2%. A total of 2574 frames were collected. Final cell constants were obtained from the *xyz* centroids of 9303 reflections after integration.

From the systematic absences and the observed metric constants and intensity statistics, space group $P2_1/c$ was chosen initially; subsequent solution and refinement confirmed the correctness of this choice. The structure was solved using *SIR92* and subsequent electron-density difference syntheses.[28] Refinement (full-matrix least squares) was carried out using the Oxford University *Crystals for Windows* program.[29] All ordered non-H atoms were refined using anisotropic displacement parameters. Disorder was present in one of the isopropyl groups and methyl atoms C(320) and C(321). The asymmetric unit also contained two molecules of pentane; in one of the solvate molecules, the methylene atoms C(611) and C(610) were disordered. Thus, the sum of occupancies of the constituent atoms involved in the disorder were constrained to sum to 1.0. The value of the occupancy for the major methyl atom C(320) was 0.796(5), while the value of the occupancy for the major methylene atom C(611) was 0.593(7). The disordered C atoms were refined using isotropic displacement parameters. After location of H atoms on electron-density difference maps, the H atoms were initially refined with soft restraints on the bond lengths and angles to regularize their geometry (C---H in the range 0.93−0.98 Å and U_{iso}(H) in the range 1.2−1.5U_{eq} of the parent atom), after which the positions were refined with riding constraints.[30] The final least-squares refinement converged to R1 = 0.0294 [$I > 2\sigma(I)$; 11249 data] and wR2 = 0.0698 [F^2; 14734 data; 631 parameters]. The final CIF file is available as Supporting Information; we note that the CheckCIF routine produced one Alert B item, related to a disorder discussed above. Accordingly, the CIF file and CheckCIF output contain a validation reply form item that addresses the Alert B item.

■ ASSOCIATED CONTENT

Ⓢ Supporting Information

Graphical depictions of the variable-temperature NMR spectra of TH**1**, coordinate files of DFT-calculated structures, and CIF files for ^{F}**1** and TH**1**. This material is available free of charge via the Internet at http://pubs.acs.org.

■ AUTHOR INFORMATION

Corresponding Author

*E-mail: ozerov@chem.tamu.edu.

Notes

The authors declare no competing financial interest.

dx.doi.org/10.1021/ic301629m | *Inorg. Chem.* 2013, 52, 2317−2322

■ ACKNOWLEDGMENTS

Support of this research by the U.S. National Science Foundation (through Grants CHE-0517798, CHE-0809522, and CHE-0944634 to O.V.O., through Grant CHE-0521047 for the purchase of a diffractometer at Brandeis University, and through Grant CHE-0910552 to M.B.H.), the Welch Foundation (Grant A-1717), the Alfred P. Sloan Foundation (Research Fellowship to O.V.O.), and the Dreyfus Foundation (Camille Dreyfus Teacher−Scholar Award to O.V.O.) is gratefully acknowledged. We also thank Prof. G. Parkin for a productive discussion of the subject of this paper.

■ REFERENCES

(1) Huacuja, R.; Graham, D. J.; Fafard, C. M.; Chen, C.-H.; Foxman, B. M.; Herbert, D. E.; Alliger, G.; Thomas, C. M.; Ozerov, O. V. *J. Am. Chem. Soc.* **2011**, *133*, 3820.

(2) Fafard, C. M.; Adhikari, D.; Foxman, B. M.; Mindiola, D. J.; Ozerov, O. V. *J. Am. Chem. Soc.* **2007**, *129*, 10318.

(3) (a) Liang, L.-C.; Lin, J.-M.; Hung, C.-H. *Organometallics* **2003**, *22*, 3007. (b) Winter, A. M.; Eichele, K.; Mack, H.-G.; Potuznik, S.; Mayer, H. A.; Kaska, W. C. *J. Organomet. Chem.* **2003**, *682*, 149.

(4) Fan, L.; Foxman, B. M.; Ozerov, O. V. *Organometallics* **2004**, *23*, 326.

(5) For reviews on the chemistry of diarylamido-based PNP complexes, see: (a) Liang, L.-C. *Coord. Chem. Rev.* **2006**, *250*, 1152. (b) Ozerov, O. V. In *The Chemistry of Pincer Compounds*; Morales-Morales, D., Jensen, C., Eds.; Elsevier: Amsterdam, The Netherlands, 2007; pp 287−309. (c) Mindiola, D. J.; Bailey, B. C.; Basuli, F. *Eur. J. Inorg. Chem.* **2006**, 3135.

(6) Rohmer, M.-M.; Bénard, M. *Chem. Soc. Rev.* **2001**, *30*, 340.

(7) (a) Feng, Q.; Rauchfuss, T. B.; Wilson, S. R. *J. Am. Chem. Soc.* **1995**, *117*, 4702. (b) Halfen, J. A.; Mahapatra, S.; Wilkinson, E. C.; Kaderli, S.; Young, V. G., Jr.; Que, L., Jr.; Zuberbühler, A. D.; Tolman, W. B. *Science* **1996**, *271*, 1397. (c) Niecke, E.; Fuchs, A.; Nieger, M. *Angew. Chem., Int. Ed.* **1999**, *38*, 3028. (d) Rodriguez, A.; Olsen, R. A.; Ghaderi, N.; Scheschkewitz, D.; Tham, F. S.; Mueller, L. J.; Bertrand, G. *Angew. Chem., Int. Ed.* **2004**, *43*, 4880.

(8) (a) Hunter, B. M.; Villahermosa, R. M.; Exstrom, C. L.; Hill, M. G.; Mann, K. R.; Gray, H. B. *Inorg. Chem.* **2012**, *51*, 6898. (b) Hartsock, R. W.; Zhang, W.; Hill, M. G.; Sabat, B.; Gaffney, K. G. *J. Am. Chem. Soc.* **2012**; *J. Phys. Chem. A* **2011**, *115*, 2920. (c) Kolle, U.; Kossakowski, J.; Klaff, N.; Wesemann, L.; Englert, U.; Heberich, G. E. *Angew. Chem., Int. Ed. Engl.* **1991**, *30*, 690. (d) Exstrom, C. L.; Britton, D.; Mann, K. R.; Hill, M. G.; Miskowski, V. M.; Schaefer, W. P.; Gray, H. B.; Lamanna, W. M. *Inorg. Chem.* **1996**, *35*, 549.

(9) These have sometimes been called "deformational isomers": Parkin, G.; Hoffmann, R. *Angew. Chem., Int. Ed. Engl.* **1994**, *33*, 1462.

(10) Weng, W.; Guo, C.; Moura, C. P.; Yang, L.; Foxman, B. M.; Ozerov, O. V. *Organometallics* **2005**, *24*, 3487.

(11) Weng, W.; Guo, C.; Çelenligil-Çetin, R.; Foxman, B. M.; Ozerov, O. V. *Chem. Commun.* **2006**, 197.

(12) Fafard, C. M.; Chen, C.-H.; Foxman, B. M.; Ozerov, O. V. *Chem. Commun.* **2007**, 4465.

(13) Fan, L.; Yang, L.; Guo, C.; Foxman, B. M.; Ozerov, O. V. *Organometallics* **2004**, *23*, 4778.

(14) (c) Lin, W.; Wilson, S. R.; Girolami, G. S. *Inorg. Chem.* **1994**, *33*, 2265.

(15) Kullberg, M. L.; Lemke, F. R.; Powell, D. R.; Kubiak, C. P. *Inorg. Chem.* **1985**, *24*, 3589.

(16) (a) Gorlov, M.; Fischer, A.; Kloo, L. *Inorg. Chim. Acta* **2009**, *362*, 605. (b) Akerstedt, J.; Gorlov, M.; Fischer, A.; Kloo, L. *J. Organomet. Chem.* **2010**, *695*, 1513. (c) Smith, D. A.; Batsanov, A. S.; Costuas, K.; Edge, R.; Apperley, D. C.; Collison, D.; Halet, J.-F.; Howard, J. A. K.; Dyer, P. W. *Angew. Chem., Int. Ed.* **2010**, *49*, 7040.

(17) Dotta, P.; Kumar, P. G. A.; Pregosin, P. S.; Albinati, A.; Rizzato, S. *Organometallics* **2004**, *23*, 4247.

(18) POV-Ray—The Persistence of Vision Raytracer, available at http://www.povray.org/.

(19) ORTEP plots were created using *Ortep-3 for Windows*: Farugia, L. *J. Appl. Crystallogr.* **1997**, *30*, 565.

(20) All data were collected at 120 K using Mo Kα (0.71073 Å) radiation. Data refinement was performed using full-matrix least squares on F^2 and multiscan absorption corrections.

(21) Stephens, P. J.; Devlin, F. J.; Chabalowski, C. F.; Frisch, M. J. *J. Phys. Chem.* **1994**, *98*, 11623.

(22) Becke, A. D. *J. Chem. Phys.* **1993**, *98*, 5648.

(23) Lee, C.; Yang, W.; Parr, R. G. *Phys. Rev. B* **1988**, *37*, 785.

(24) Frisch, M. J.; Trucks, G. W.; Schlegel, H. B.; Scuseria, G. E.; Robb, M. A.; Cheeseman, J. R.; Scalmani, G.; Barone, V.; Mennucci, B.; Petersson, G. A.; Nakatsuji, H.; Caricato, M.; Li, X.; Hratchian, H. P.; Izmaylov, A. F.; Bloino, J.; Zheng, G.; Sonnenberg, J. L.; Hada, M.; Ehara, M.; Toyota, K.; Fukuda, R.; Hasegawa, J.; Ishida, M.; Nakajima, T.; Honda, Y.; Kitao, O.; Nakai, H.; Vreven, T.; Montgomery, J. A., Jr.; Peralta, J. E.; Ogliaro, F.; Bearpark, M.; Heyd, J. J.; Brothers, E.; Kudin, K. N.; Staroverov, V. N.; Kobayashi, R.; Normand, J.; Raghavachari, K.; Rendell, A.; Burant, J. C.; Iyengar, S. S.; Tomasi, J.; Cossi, M.; Rega, N.; Millam, J. M.; Klene, M.; Knox, J. E.; Cross, J. B.; Bakken, V.; Adamo, C.; Jaramillo, J.; Gomperts, R.; Stratmann, R. E.; Yazyev, O.; Austin, A. J.; Cammi, R.; Pomelli, C.; Ochterski, J. W.; Martin, R. L.; Morokuma, K.; Zakrzewski, V. G.; Voth, G. A.; Salvador, P.; Dannenberg, J. J.; Dapprich, S.; Daniels, A. D.; Farkas, O.; Foresman, J. B.; Ortiz, J. V.; Cioslowski, J.; Fox, D. J. *Gaussian 09*, revision B.01; Gaussian, Inc.: Wallingford, CT, 2009.

(25) (a) Hehre, W. J.; Ditchfield, R.; Pople, J. A. *J. Chem. Phys.* **1972**, *56*, 2257. (b) McLean, A. D.; Chandler, G. S. *J. Chem. Phys.* **1980**, *72*, 5639. (c) Frisch, M. J.; Pople, J. A.; Binkley, J. S. *J. Chem. Phys.* **1984**, *80*, 3265.

(26) Kuechle, W.; Dolg, M.; Stoll, H.; Preuss, H. *J. Chem. Phys.* **1994**, *100*, 7535.

(27) *Apex2, User Manual*, version 2; M86-E01078; Bruker Analytical X-ray Systems: Madison, WI, June 2006.

(28) Altomare, A.; Cascarano, G.; Giacovazzo, G.; Guagliardi, A.; Burla, M. C.; Polidori, G.; Camalli, M. *J. Appl. Crystallogr.* **1994**, *27*, 435.

(29) Betteridge, P. W.; Carruthers, J. R.; Cooper, R. I.; Prout, K.; Watkin, D. J. *J. Appl. Crystallogr.* **2003**, *36*, 1487. Watkin, D. J.; Prout, C. K.; Pearce, L. J. *CAMERON*; Chemical Crystallography Laboratory: Oxford, U.K., 1996.

(30) Cooper, R. I.; Thompson, A. L.; Watkin, D. J. *J. Appl. Crystallogr.* **2010**, *43*, 1100−1107.